Spin-liquid phase of the multiple-spin exchange Hamiltonian on the triangular lattice

G. Misguich, C. Lhuillier, and B. Bernu
Laboratoire de Physique Théorique des Liquides–UMR 7600 of CNRS, Université Pierre et Marie Curie, case 121, 4 Place Jussieu, 75252 Paris Cedex, France

C. Waldtmann
Institut für Theoretische Physik, Universität Hannover, D-30167 Hannover, Germany
(Received 21 December 1998)

We performed an exact diagonalization study of the spin-liquid phase of the multiple-spin exchange model on a triangular lattice. It is characterized by no Néel long-range order, short-ranged magnetic correlations, and a spin gap. We found no long-range order in any local order parameter we investigated (chiral, dimer, etc.) The probable asymptotic ground-state degeneracy is discussed. We argue that it could be of topological origin and that the system is probably not a chiral spin liquid. A possible relation to the Affleck-Kennedy-Lieb-Tasaki, or valence-bond solid phase is discussed. [S0163-1829(99)15125-7]

I. INTRODUCTION

A general model. The multiple-spin exchange (MSE) model was introduced by Thouless.[1] It is an effective description of the magnetic properties of quasilocalized fermions. This lattice spin Hamiltonian was introduced to describe the magnetic consequences of tunneling events where several indistinguishable particles exchange their positions. For spin-$\frac{1}{2}$ particles, when two-body processes are the only important events, it leads to the familiar Heisenberg Hamiltonian

$$H=\sum_{i<j} J_{i,j}P_{i,j}=\sum_{i<j} J_{i,j}\left(2\vec{S}_i\cdot\vec{S}_j+\frac{1}{2}\right), \tag{1}$$

where $P_{i,j}$ is the spin permutation operator and $2J_{i,j}$ the (positive) frequency of the tunnel process exchanging the particle on site i and the particle on site j. But in low-density crystals, cyclic exchange processes P_n of $n\geqslant 3$ particles can be important. It is the case in low-density solid ^{3}He films (Ref. 2 and references therein) and in the Wigner crystal.[3] More generally, multiple-spin interactions with $n\geqslant 2$ are expected in spin systems where interactions are strong and cannot be reduced to Heisenberg couplings. In numerous quantum crystals, such couplings are expected to be generated by integrating out the nonmagnetic degrees of freedom. For instance, the role played by MSE in the context of metal-insulator transitions has been discussed recently by Chakravarty *et al.*[4] Therefore it is of wide interest to understand the nature of the magnetic fluctuations introduced by MSE couplings.

The MSE spin-liquid phase. In a previous work we studied the phase diagram of the MSE model on a triangular lattice and showed the existence of a spin-liquid phase.[5] In this work we present a detailed characterization of the low-energy physics of this new spin liquid. The Hamiltonian involves the five simplest ring exchange patterns on the triangular lattice:

$$H = J_2 \sum_{\bullet\!-\!\bullet} P_2 - J_3 \sum_{\triangle} \left(P_3+P_3^{-1}\right) + J_4 \sum_{\diamond} \left(P_4+P_4^{-1}\right) - J_5 \sum_{\diamond\!\!\!\!\diamond} \left(P_5+P_5^{-1}\right) + J_6 \sum_{\hexagon} \left(P_6+P_6^{-1}\right). \tag{2}$$

Due to the Pauli principle, exchange of an odd number of fermions is ferromagnetic whereas exchange of an even number is antiferromagnetic. This is the reason for the alternating signs in Eq. (2) (all J_n being >0). Because of the equality $P_{1,2,3}+P_{3,2,1}=P_{1,2}+P_{2,3}+P_{3,1}-1$, valid for spin $\frac{1}{2}$, triple exchange around triangles can be taken into account just by modifying the bare J_2 frequency $J_2\rightarrow J_2-2J_3$. In the following we thus assume without any loss of generality that $J_3=0$ and that J_2 can be $\geqslant 0$ or <0.

At $T=0$ there is a first-order phase transition between a paramagnetic phase (the ground state is a singlet $S=0$) and a ferromagnetic one (the ground state is fully polarized: $S=N/2$).[5] In this work we are interested in the ground-state and first-excited-state structure in the paramagnetic phase. The behavior of this spin liquid when an external magnetic field is applied will be discussed elsewhere.[33,42]

What kind of spin liquid is the MSE model? Many different quantum ground states, which differ by their spatial broken symmetries and excitation spectra, have short-ranged spin-spin correlations and an $S=0$ ground state. Among the two-dimensional Hamiltonians with a single spin in the unit cell (no dimerization nor inequivalent bonds) there are three important examples where the ground-state wave function is understood.

(i) Spin-$\frac{1}{2}$ Klein[6] models. This family of Hamiltonians generalizes the Majumdar-Gosh[7] model. Since any first-neighbor valence-bond state is a ground state, the degeneracy is extensive in two dimensions.

(ii) Valence bond crystal. It has some dimer-dimer long-ranged order (LRO) or some more complicated plaquette order. It has a spin gap and spin-spin correlations are short ranged. The translation symmetry is spontaneously broken and therefore the ground state is degenerate. An example may be the frustrated antiferromagnet on the square lattice.[8,9] These spatial symmetry breakings are found in large-N limits of SU(N) models[10–12] when the spin S does not match the coordination number z ($2S \neq 0 \mod z$).

(iii) Valence bond solid (VBS) (Affleck *et al.*[13]). It exists when the spin S on one site matches the z coordination number of the lattice ($2S=z$). It breaks no symmetry and has a spin gap but, *a priori*, it cannot be constructed with spin $\frac{1}{2}$. The Haldane phase[14] in one dimension (integer spin) belongs to the same universality class. The ground state is nondegenerate (infinite-volume limit with periodic boundary conditions); spin-spin and dimer-dimer correlations decay exponentially with distance.

There are very few models where resonances between short-ranged valence-bond states select a single (and fully symmetric under symmetry operations) combination of them. A perturbed Klein Hamiltonian could be a realization.[15] The J_1-J_2-J_3 model on the square lattice might also be a candidate (exact diagonalizations on a $N=16$ sample[16]). So far, the short-ranged resonating valence-bond (RVB) picture proposed by Anderson[17] has not yet found an explicit realization: there is no definite spin-$\frac{1}{2}$ Hamiltonian in two dimensions with no broken translation symmetry and a nondegenerate ground state. From this point of view MSE is of great relevance since our numerical data point to short-ranged correlations with no kind of LRO.

II. RANGE OF THE SPIN-LIQUID PHASE IN THE MSE MODEL ON A TRIANGULAR LATTICE

Even in the classical limit, the ground state of the MSE Hamiltonian is exactly known only in three limits.

(i) Pure $J_2>0$ case: three-sublattice Néel state.

(ii) Pure J_4 case: four-sublattice Néel state (tetrahedral state found by Momoi, Kubo, and Niki[18,19]).

(iii) Pure J_n with odd n: ferromagnetic.

An approximate phase diagram for the classical system at $T=0$ has been obtained in the variational subspace of planar helices[20] and in the four-sublattice subspace for the J_2-J_4 model (Kubo and Momoi[18]). From these results we can sketch the *qualitative* shape of the classical diagram (dotted line of Fig. 1).

In the $S=\frac{1}{2}$ quantum system there is hardly any exact result, but some regions of the diagram are understood.

(i) Pure $J_2>0$ case: the antiferromagnetic (AF) Heisenberg Hamiltonian has three-sublattice Néel LRO (NLRO).[21]

(ii) Large region about the pure J_4 case: no LRO, finite spin gap, and short-ranged spin-spin correlations.[5]

(iii) Large ferromagnetic phase including the pure $J_2<0$ and pure J_5 Hamiltonians.

A possibility for the quantum phase diagram is presented in Fig. 1. This simple guess relies on the following data.

(i) Preliminary exact diagonalization results indicate that the extension of three-sublattice Néel phase in the J_2-J_4 model is strongly reduced by four-spin exchange. This is already the case at the mean-field Schwinger-boson level.[20]

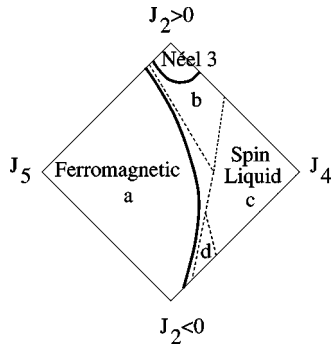

FIG. 1. Qualitative phase diagram of the MSE model on the triangular lattice. The right corner is the pure J_4 model; the left one is the pure J_5 one. Down and up corners are the ferromagnetic and antiferromagnetic Heisenberg Hamiltonians. Letters and dashed lines: Schematic phase diagram for the classical model. *a*, Ferromagnetic; *b*, three-sublattice Néel state; *c*, four-sublattice Néel state; *d*, long-wavelength spiral state or ferrimagnetic state. Solid lines: likely scenario for the $S=\frac{1}{2}$ quantum phase. We put a small disordered window on the upper $J_4=0$ line but a first-order transition between ferromagnetism and three-sublattice Néel order is also possible; some more numerical work is needed to fix this point.

The possibility that this Néel phase is destroyed by an infinitely small J_4 is not excluded (additional work is in progress).

(ii) Our exact diagonalization data show no LRO in the large-J_4 region.

(iii) The energy of the ferromagnetic state is the same in the classical and quantum cases but AF configurations gain energy from quantum fluctuations. Therefore, the ferromagnetic phase is slightly reduced in the $S=\frac{1}{2}$ case.

On the J_2- (>0) J_5 line, we suggest the existence of a spin-liquid window between the ferromagnetic and the three-sublattice Néel phase. However, this has not yet been numerically investigated. Another possibility is a first-order phase transition between NLRO and ferromagnetism.

III. SHORT-RANGED MAGNETIC CORRELATIONS

A. No Néel long-range order

The first question to address in the nonferromagnetic region is, is the system Néel long-range ordered at $T=0$?

Periodic boundary conditions. As a Néel state breaks the SU(2) and some spatial symmetries of H, it cannot be an exact eigenstate on a finite size system. It has to be a linear combination of eigenstates belonging to different irreducible representations (IR's) of the spatial symmetry group and to different S sectors.[21,22] As the dynamics of a Néel order parameter is the one of a free rotator, the corresponding low-energy levels scale as

$$E \simeq \frac{S(S+1)}{N\chi_0} \tag{3}$$

since the inertia of that rotator is proportional to the number of sites, N [χ_0 is the susceptibility per site at zero field: $\chi_0 = (1/N)\partial\langle 2S\rangle/\partial B_{|B=0}$]. At fixed S, these states collapse to the ground state in thermodynamic limit more rapidly than the softest magnon.[23] These states form a *tower of states*. This low-energy structure is absent in the spectra as soon as

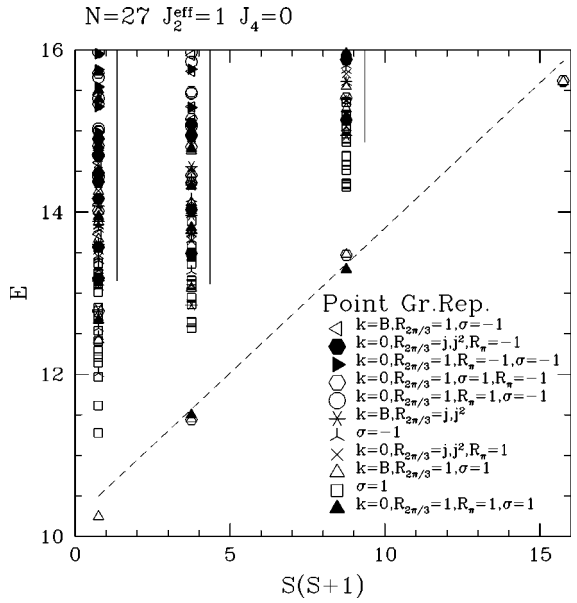

FIG. 2. First-neighbor Heisenberg spectrum on the triangular lattice. The SU(2) and spatial symmetry breakings due to the three-sublattice long-range Néel order appear as a set of states with an energy scaling as $E(S)\sim S(S+1)/N$ (dashed line). The symbols represent the quantum number of the different eigenstates. **k** is the wave vector. $\mathbf{k}=B$ is the corner of the Brillouin zone (the impulsion is not indicated if $\mathbf{k}\neq 0$ and $\neq B$). R_θ is the phase factor obtained in a θ rotation about the origin and σ stands for a reflection about an axis. The vertical lines indicate the energy range where the density of states is high and all the eigenvalues have not been computed. This has no consequence on the low-energy part of each irreducible representation of the symmetry group, where the eigenstates are known exactly.

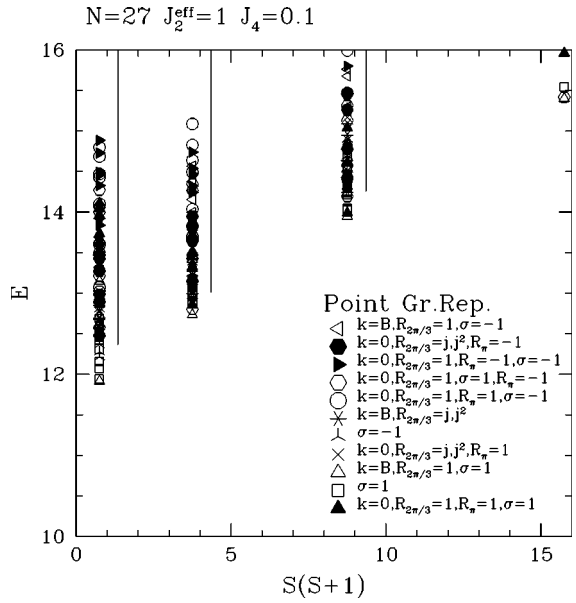

FIG. 3. Heisenberg spectrum perturbed with four-body exchange $J_4/J_2=0.1$. The Néel structure is destroyed: the states formerly embedding the symmetry breakings in the $J_4=0$ case have been ''pushed up'' in energy to the continuum of excitations.

J_4 is not negligible. Figures 2 and 3 show how the three-sublattice Néel tower of state is destroyed by four-spin exchange.

Twisted boundary conditions. For the tower of states to appear on a finite-size sample, the sublattice structure must be compatible with the boundary conditions. An order with a long-wavelength helix or an incommensurate phase is therefore difficult to detect on small samples with periodic boundary conditions. Fortunately, twisted boundary conditions[24] allow us to overcome this difficulty.[21] For $N=19$ and $J_2=-2$, $J_4=1$, we scanned the Brillouin zone to determine the twist $\mathbf{q}_0$ which minimizes the ground-state energy. The twist vector $\mathbf{q}_0$ lies inside the Brillouin zone and has no particular symmetry. If the system had some NLRO (commensurate or not), this $\mathbf{q}_0$ would indicate the ordering wave vector and the spectrum would show a tower of states $E\simeq(S^z)^2/N\chi_\perp$. Figure 4 shows that it is not the case.

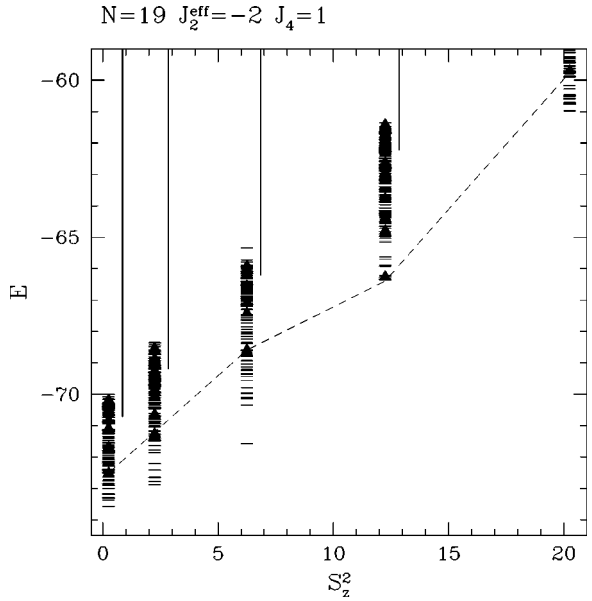

FIG. 4. Spectrum with the twisted boundary conditions which minimize the ground-state energy. Eigenstates represented by black triangles are $\mathbf{k}=\mathbf{0}$ states. The spectrum shows no long-ranged (spiral) order: if there was a *tower of states*, the lowest $\mathbf{k}=\mathbf{0}$ states (joined by the dashed line) would be lower than the other excitations and their energies would be proportional to S_z^2. Notice that with these twisted boundary conditions the spatial symmetries (except translations) as well as the SU(2) symmetry are lost. But S_z is still a conserved quantity. The twist vector is $\mathbf{q}_0=0.27\mathbf{A}_1-0.20\mathbf{A}_2$, where $\mathbf{A}_1$ and $\mathbf{A}_2$ are middle of the boundary of the Brillouin zone. By symmetry, there are twelve twists equivalent to $\mathbf{q}_0$.

B. Spin-spin correlations $\langle\vec{S}_i\cdot\vec{S}_j\rangle$

For spin-$\frac{1}{2}$, $\vec{S}_i\cdot\vec{S}_j$ varies between $-3/4$ (singlet) and 1/4 (triplet) and the statistical average is zero. Compared to these extremal values, the spin-spin correlations measured in the ground state of $J_2=-2$, $J_4=1$ for $N=16$, 24, and 28 are small (Table I). Figure 5 displays the absolute value of the spin-spin correlation as a function of distance. On these three samples the available distances are rather small ($|i-j|\leqslant 3$)

TABLE I. Correlations $\langle \vec{S}_i \cdot \vec{S}_j \rangle$ in the MSE ground state of $N=16$, 24, and 28 samples ($J_2=-2$, $J_4=1$). These data are plotted in Fig. 5. The $N=24$ sample is a 6×4 lattice which does not have the $\mathcal{R}_{2\pi/3}$ symmetry. The three directions are thus nonequivalent; this explains why $\langle \vec{S}_i \cdot \vec{S}_j \rangle$ has three possible values at distance 1. The underlined values are overcorrelated due to periodic boundary conditions: they correspond to antipodal sites on the torus.

$\|i-j\|$	$N=28$	$N=24$			$N=16$
1	−0.06941	−0.08925	−0.06356	−0.04894	-0.06614
$\sqrt{3}$	−0.08014	−0.11194	−0.03425	−0.01640	−0.02887
2	−0.02534	−0.17823	−0.02560	+0.02051	−0.05996
$\sqrt{7}$	+0.04983	+0.07542	+0.00306	−0.00454	×
3	×		+0.01471		×

and the data show important size and orientation dependence (for $N=24$, the system has no $\mathcal{R}_{2\pi/3}$ symmetry and there are three nonequivalent directions).

At this point, it is difficult to draw conclusions on the spin-spin correlation decay from Fig. 5. However, a finite-size system with periodic boundary conditions is a torus and we expect some geometrical effects for pairs (i,j) of sites which have particular symmetries. The strongest effect is the enhancement of $\langle \vec{S}_i \cdot \vec{S}_j \rangle$ on samples where $\mathbf{j}-\mathbf{i}$ and $\mathbf{i}-\mathbf{j}$ are equivalent vectors: antipodal sites are overcorrelated (underlined values in Table I). If the sample has no $\mathcal{R}_{2\pi/3}$ symmetry, the finite-size effect on $\langle \vec{S}_i \cdot \vec{S}_j \rangle$ at distance $d=|i-j|$ should be weaker in the direction of the vector $\mathbf{v}=\mathbf{i}-\mathbf{j}$ which is not frustrated by the periodicity of the torus.[25] If we eliminate antipodal sites and frustrated directions in $N=24$ only the solid symbols of Fig. 5 remain. The behavior looks more regular and the rapid decay suggests a rather short correlation length.

The point is now to understand the local structure of the ground-state wave function. There are two naive ways to build an $S=0$ state out of a large number of spins $\frac{1}{2}$: (1) combine ferromagnetically the spins in a small number of sublattices (NLRO) and let these large spins screen themselves or (2) combine the spins two by two in singlets. The absence of a tower of states and significant ferromagnetic correlations has excluded the first possibility (no NLRO). It is easy to check that the weakness of the AF correlations makes the second scenario unlikely: the screening of a single spin at the origin involves an important number of neighbors, up to distance $d\simeq2$–3. (This is easily checked from the data of Table I.) This will be confirmed in the next subsection where we show that dimer-dimer correlations are weak.

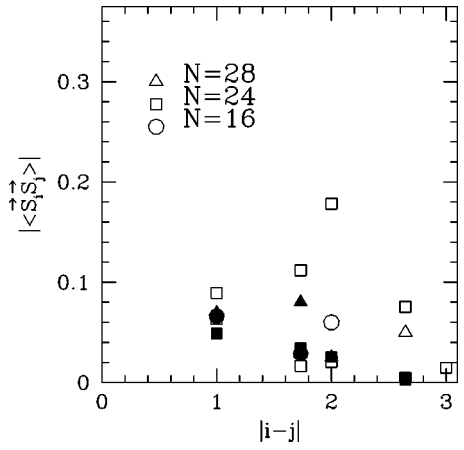

FIG. 5. Absolute value of the spin-spin correlation (data of Table I). The vertical range goes from 0 to $\frac{3}{8}$. $-\frac{3}{8}$ is the first-neighbor correlation in the Majumdar-Gosh chain. These scales have been chosen to show how small the correlations are in the MSE system. The solid symbols correspond to correlations for which finite-size effects are expected to be the smallest (see text).

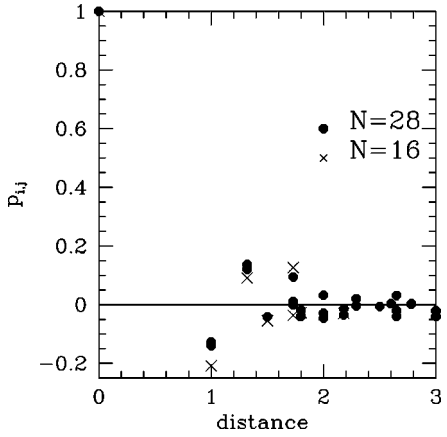

FIG. 6. Dimer-dimer correlations in the ground state $|\Psi\rangle$ of the MSE Hamiltonian in the spin-liquid phase ($J_2=-2$ and $J_4=1$). They are plotted as a function of distance between bonds for $N=16$ and 28.

C. Dimer-dimer correlations

We define the dimer operator on a pair of sites (i,j) by $d_{i,j}=(1-P_{i,j})/2$. This projector is 1 on a singlet and 0 on a triplet. The dimer correlation between a reference bond (1,2) and (i,j) is $D_{i,j}=\langle\Psi|d_{1,2}d_{i,j}|\Psi\rangle-\langle\Psi|d_{1,2}|\Psi\rangle\langle\Psi|d_{i,j}|\Psi\rangle$.[26] As for the normalization, we look for the maximum value of $D_{i,j}$. It is achieved when the two bonds are completely correlated and gives $D_{i,j}=\langle\Psi|d_{1,2}|\Psi\rangle-\langle\Psi|d_{i,j}|\Psi\rangle\langle\Psi|d_{1,2}|\Psi\rangle$. So we measure dimer correlations by

$$p_{i,j}=\frac{D_{i,j}}{\langle\Psi|d_{1,2}|\Psi\rangle(1-\langle\Psi|d_{i,j}|\Psi\rangle)}=\frac{\langle\Psi|d_{1,2}d_{i,j}|\Psi\rangle-\langle\Psi|d_{i,j}|\Psi\rangle\langle\Psi|d_{1,2}|\Psi\rangle}{(1-\langle\Psi|d_{i,j}|\Psi\rangle)\langle\Psi|d_{1,2}|\Psi\rangle}. \quad (4)$$

$p_{i,j}$ is represented in Figs. 6 and 7. For this quantity, zero means that the presence of a singlet on (1,2) and the presence of a singlet on (i,j) are uncorrelated. A value of 1 means that if a singlet exists on (1,2), there is always one on (i,j). The minimal possible value is $p_{i,j}^{\min}=-\langle d_{i,j}\rangle/(1-\langle d_{i,j}\rangle)$, which is $p_{i,j}^{\min}=-0.469$ at distance 1 in the $N=28$ ground state. We observe negative values on the four bonds which are at a distance 1 from the reference bond. Compared to $p_{i,j}^{\min}$, these values are important (30%) and increase with the system size. This testifies to an important short-ranged repulsion of parallel dimers and excludes the possibility of spin-Peierls-like structures in which the lattice would be regularly tiled with parallel dimers. Figure 7 shows

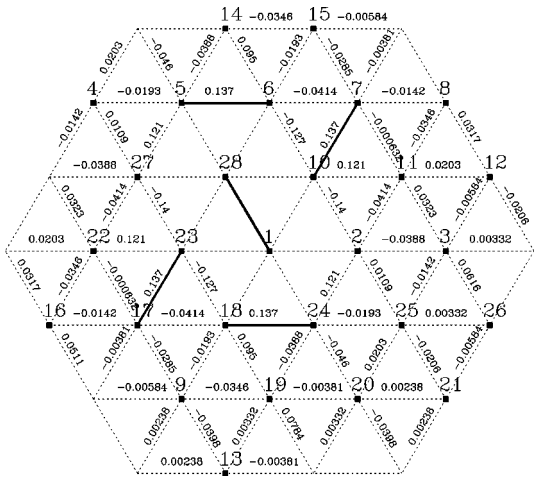

FIG. 7. Values of $p_{i,j}$ on the $N=28$ lattice: the reference bond is (1,28) and the four most strongly correlated bonds are in the solid line; they are at distance $d=\sqrt{7}/2$ from (1,28) and form a triangular pattern. We notice that the four ''first neighbors'' of the bond (1,28) are strongly anticorrelated [see values on (6,10) (10,2) (23,27), and (18,23)].

that the local dimer distribution favors an angle of $\pm\pi/3$ between dimers bonds. This tendency to a $\pm\pi/3$ ordering of dimers already appears in the six-site system with open boundary conditions. This system (shape of a triangle) is the smallest system with a low ground-state energy and a significant spin gap. In larger systems, this local $\pm\pi/3$ structure is all the more pronounced as the ground-state energy is low.

From Fig. 6 one could doubt that the dimer-dimer correlation goes to zero with distance. However, we think it is the case for the following reasons: (1) Dimer-dimer correlations are very weak. Even at short distances, the wave function has to be seen as a gas or a liquid and not as solid of dimers. (2) The correlation at distances $d\geqslant 2$ decreases in a significant way from $N=24$ to $N=28$. (3) It is not possible to tile the triangular lattice with dimers at $\pm\pi/3$ from their neighbors without defaults (one site out of seven would not touch any dimer; see Fig. 8) and this *local* property cannot be propagated to the entire lattice. We stress that this $\pm\pi/3$ dimer correlation cannot picture the entire wave function. It would not account for the low first-neighbor ''dimer density'': $\langle\vec{S}_i\cdot\vec{S}_j\rangle$ at a distance $|i-j|=1$ is only very weakly antiferromagnetic ($\langle\vec{S}_i\cdot\vec{S}_j\rangle\simeq-0.07$), and for $N=28$, $\langle d_{1,2}\rangle$ is even lower than the second-neighbor one $\langle d_{1,11}\rangle$; see Table I. The information provided by the dimer structure of Fig. 7 is that a low-energy state cannot be achieved without a local order with a complex geometry.

D. Chiral-chiral correlations $\langle \mathrm{Im}(P_{i,j,k})\mathrm{Im}(P_{i',j',k'})\rangle$

Kubo *et al.* have demonstrated that the classical ground state of the $J_4=1$ Hamiltonian is a four-sublattice Néel state, where the magnetization vectors of the four sublattices form a regular tetrahedron.[18,19] Momoi *et al.* showed with Monte Carlo simulations that the *classical* system has a chiral phase transition at finite temperature.[19] This transition is associated with the ferromagnetic Ising-like order parameter defined on three sites by the operator $\kappa=2(\vec{S}_1\times\vec{S}_3)\cdot\vec{S}_2$. In the classical ground state all triangles have a chirality $\kappa=+\sqrt{3}/9$ or $\kappa=-\sqrt{3}/9$. Momoi's simulations indicate that the $\langle\kappa_{(1,2,3)}\kappa_{(1',2',3')}\rangle$ correlation function remains long ranged up to a finite critical temperature. To check this hypothesis in the quantum case, we have computed this correlation in the ground state of the *quantum* system for the pure J_4 Hamiltonian (like Momoi *et al.*) and found a significant decay with distance (Fig. 9). Moreover, this correlation shows negative values, which is unexpected for a ferromagnetic Ising model. The existence of such Ising LRO in the quantum system, even at $T=0$, seems unlikely.

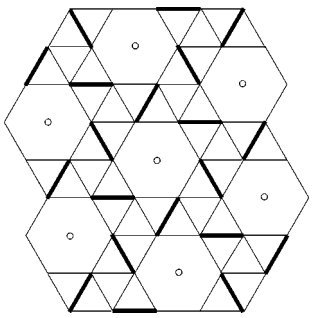

FIG. 8. Dimer covering of a 6/7-depleted triangular lattice. It is not possible to tile the triangular lattice with dimers forming angles $\pm\pi/3$ without defects. One site out of seven does not have any dimer (circles). It is worth noticing that a multiple-spin exchange Hamiltonian for which this state is an exact ground state can be constructed by the procedure introduced by Klein (Ref. 6). The Klein Hamiltonian is a sum of projectors: each projector acts on a rhombus and projects the four sites in their $S=2$ subspace. All sites are equivalent on the depleted lattice and the Hamiltonian can be expressed as a multiple-spin exchange Hamiltonian containing $P_{i,j}$ at distance 1 ($J_2=5$) and $\sqrt{3}$ ($J_2^{\mathrm{nn}}=1$) and four-body terms on a rhombus ($J_4=1$ for $P_{1,2,3,4}+\mathrm{H.c.}$ and $J_4'=2$ for a $P_{1,3}P_{2,4}$ term on the same rhombus). This state is also an eigenstate for the first-neighbor antiferromagnetic Heisenberg Hamiltonian on this lattice.

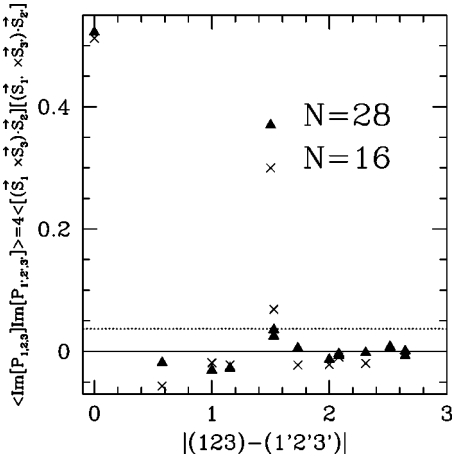

FIG. 9. Chiral-chiral correlation function for the $J_4=1$ Hamiltonian. The distance is measured in lattice spacing units between the center of gravity of the two triangles. The chirality is simply expressed with spin exchange operator $\mathrm{Im}(P_{i,j,k})=(1/2i)(P_{i,j,k}-P_{k,j,i})=2(\vec{S}_i\times\vec{S}_k)\cdot\vec{S}_j=\kappa$. The value in the classical tetrahedral state is $\langle\mathrm{Im}[P]\mathrm{Im}[P']\rangle=\frac{1}{27}\simeq 0.037$ for any couple of clockwise triangles P and P' (dotted line). If the two triangles have some sites in common, $\langle\mathrm{Im}[P]\mathrm{Im}[P']\rangle$ may have a (small) imaginary part. In this case, the real part is plotted.

TABLE II. Chiral-chiral correlation in the ground state of an $N=28$ system. $\langle \mathrm{Im}(P_{1,2,3})\mathrm{Im}(P_{1',2',3'})\rangle$ at $J_4=1$ and for two values of J_2. (1,2,3) and $(1'2'3')$ are clockwise triangles, and $|(123)-(1'2'3')|$ is the distance between the centers of the two triangles. The increase of the chirality at distance $\sqrt{7}$ is very likely to be a finite-size effect. For the three other distances we observe a significant decrease of chirality due to the first-neighbor ferromagnetic coupling ($J_2=-2$).

$\lvert(123)-(1'2'3')\rvert$	$J_2=-2,\ J_4=1$	$J_2=0,\ J_4=1$
1	−0.0285	−0.0306
$\frac{\sqrt{21}}{2^3}=1.527$	+0.0280	+0.0356
	−0.0078	−0.0132
$\sqrt{7}=2.646$	+0.0018	+0.0009

It is true that the local fluctuations of κ are large: for $N=28$ $(T=0)$, $\langle\kappa^2\rangle=0.5221$ which is larger than the expectation value on three *free* spins: $\mathrm{Tr}[\kappa^2]/\mathrm{Tr}[1]=0.375$. On the other hand, it is both much smaller than the maximum quantum value of κ^2 $(=\frac{3}{4})$ and much smaller than the value obtained in the low-lying singlets on the Kagomé lattice ($\langle\kappa^2\rangle\simeq 0.7$).[27] The last reason why the value of $\langle\kappa^2\rangle$ should not be interpreted as sufficient evidence of T symmetry breaking is that it contains no information but the first-neighbor correlation

$$\langle\kappa^2\rangle=\frac{3}{2}\left(\frac{1}{4}-\langle\vec{S}_i\cdot\vec{S}_j\rangle\right). \tag{5}$$

We also performed computations at the $J_2=-2$ and $J_4=1$ points. Unsurprisingly, the ferromagnetic coupling reduces the chirality. In the ground state of $N=28$ at $J_4=1$ and $J_2=-2$ we found $\langle\kappa^2\rangle=0.4791$. This is readily understood from Eq. (5). Since $\langle\vec{S}_i\cdot\vec{S}_j\rangle$ is enhanced by a negative J_2, local fluctuations of chirality are reduced. It is more interesting to look at $\langle \mathrm{Im}[P]\mathrm{Im}[P']\rangle$ as a function of distance. The data are shown in Table II and support the absence of long-ranged chiral order at the $J_2=-2$ and $J_4=1$ points as at the pure J_4 point.

IV. LOW-ENERGY SPECTRAL PROPERTIES

In the previous section we have reported some correlation data showing that the ground-state wave function of the MSE Hamiltonian in the spin-liquid phase has short-ranged correlation functions. We now describe the low-energy spectrum of the system. We emphasize on the spin gap and the broken symmetries. Again, we concentrate on the $J_2=-2$, $J_4=1$ Hamiltonian.

A. Spin gap

1. Finite-size effects on the ground-state energy

For small sizes the spin gap and ground-state energy are sensitive to the sample shape and size. For this reason, an $N=\infty$ extrapolation of the spin gap value is not straightforward and requires a precise analysis. The apparently irregular behavior of the spin gap and ground-state energy for systems with less than $N\simeq 24$ sites (Fig. 10) indicates the short-ranged rigidity of the ground-state wave function. This agrees with the previous section: the characteristic length ξ of the ground-state correlations is a few lattice sites, and for systems of this size, the spectrum is sensitive to boundary conditions. This effect can be used to probe the local structure of the ground-state wave function and to identify some short-wavelength resonances which lower its energy. Two families of samples should be distinguished: systems with even N have a low ground-state energy and a higher spin gap than the systems with N odd. Within each family, the behavior with the size is more or less monotonous: for even-N (odd-N) systems the energy per site increases (decreases) with N and the spin gap decreases (increases) with N. The importance of a six-site periodicity for achieving a low energy[28] agrees with the $\pm\pi/3$ orientation found by looking at the short-ranged dimer-dimer correlations (Fig. 7). The enhancement of this $\pm\pi/3$ structure in the lowest-energy systems shows that it captures some important short-distance correlations.

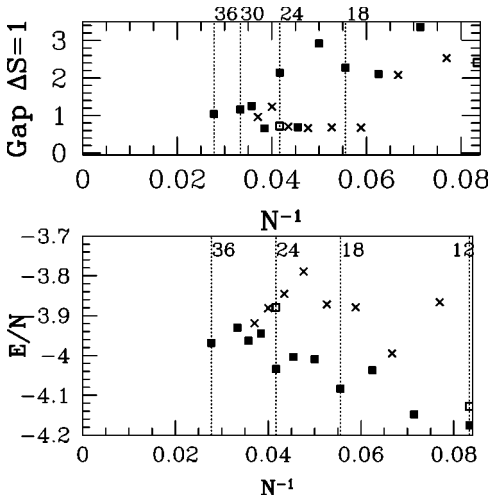

FIG. 10. Energy and spin gap for $J_2=-2$ and $J_4=1$ as a function of $1/N$. Squares: even N systems. Crosses: odd N. When different shapes have been investigated (which is the case for most sizes), only the shape with the lowest ground-state energy was plotted. The exception for $N=24$ and 12 is meant to illustrate the simultaneous decrease of the spin gap and increase of the ground-state energy when the spins are arranged in a frustrating shape.

An important point is that both families, odd and even, merge for sizes $N\geqslant N_0\simeq 30$ (either if we look at E/N or at the spin gap). We have interpreted this feature as a crossover behavior: above the characteristic size $N_0\simeq\xi^2$ the finite-size correction decays exponentially fast.[29] Figure 12 also shows a rapid decay of finite-size effects when approaching $N=36$. From this argument, the $N=36$ system can almost be considered as having reached the thermodynamic limit. This is all the more probable as this sample (6×6) has the symmetries of the infinite lattice and does not frustrate any short-ranged order that we observed to be favorable.

2. Spin gap

The correlation between the ground-state energy and the energy gap to the first $S=1$ (and $S=\frac{3}{2}$, if N is odd) excited

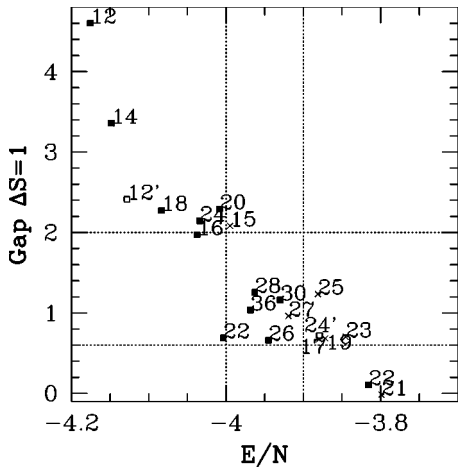

FIG. 11. Same data as in Fig. 10 with the spin gap plotted as a function of the ground state energy.

state is indeed precise (see Fig. 11): the most stable systems (i.e., with E/N minimum) are those with the largest spin gaps. The different spectra roughly fall onto one line when the spin gap is plotted versus E/N. This suggests that the position on this line is a single parameter which measures the frustration of a system. On the right part of Fig. 11, systems have important frustration, because of geometric constraints the local structure of the wave function which would minimize the energy in the infinite systems cannot develop. Systems on the left part benefit from particular boundary conditions which allow some stabilizing resonances and therefore an E/N lower than in the thermodynamic limit. From the data of E/N versus Δ we can estimate the position of the infinite system. E/N converges to -3.95 ± 0.05 (safe estimate from Fig. 10). With this energy interval, the value of the spin gap can then be extracted from Fig. 11. We obtain $\Delta=1.3\pm0.5$.

B. Ground-state symmetries in the thermodynamic limit

The spin gap described in the previous subsection ensures that in this region of the phase diagram the system does not spontaneously break SU(2) symmetry at low temperatures.

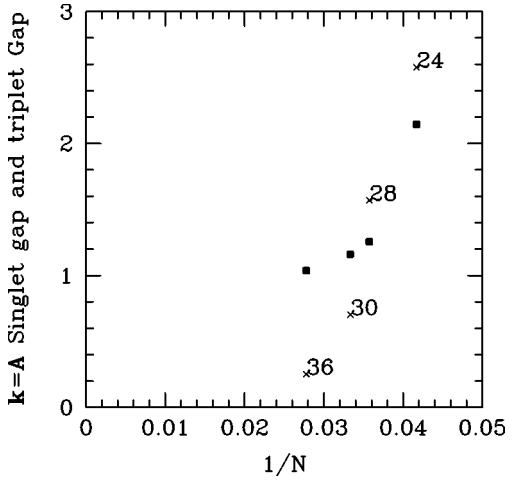

FIG. 12. Spin gap (squares) and gap to the first $\mathbf{k}=\mathbf{A}$ singlet excited state (crosses).

We now turn to the $S=0$ sector and address the question of the ground-state degeneracy and the possibility for a spatial group symmetry breaking. This is important to characterize the class of spin liquid this model belongs to.

1. Singlet states in the spin gap

In nearly all even samples ($N=36$, 30, 28, 24, 18, 16, 12) the ground state belongs to the trivial representation of the point group and translation group. This representation being one dimensional, the ground state is nondegenerate for finite N. Above the ground state we find always fewer than ten eigenstates in the spin gap (i.e., below the first triplet energy). There is no extensive entropy at $T=0$ or any singlet soft mode (notice the difference with the Kagomé lattice Heisenberg antiferromagnet[27]). This implies that the system at $J_2=-2$ and $J_4=1$ is *not* a quantum critical system.

We have analyzed the (spatial) quantum numbers of the low-energy singlet states to detect if some symmetry sectors were collapsing to the absolute ground state. So far, because of the poor regularity in the symmetries, this task has only brought partial results. Here are the most important data to be understood.

(i) There is no low-energy singlet in the $\mathbf{k}=\mathbf{B}$ sector ($\pm\mathbf{B}$ are the two corners of the Brillouin zone). This excludes any three-step translation symmetry breaking. It also confirms that the $\pm\pi/3$ dimer order (Fig. 7), which looks three-step periodic, is only *local*.

(ii) The frequent occurrence of $\mathbf{k}=\mathbf{A}$ states in the spin gap suggests that such states collapse to the ground state and give a two-step translation symmetry breaking ($\mathbf{A}$ is one middle of the boundary of the Brillouin zone). In particular the energy gap between the absolute ground state and the first $\mathbf{k}=\mathbf{A}$ state drops by a factor of 10 between $N=24$ and $N=36$ (2.5 at $N=24$ and 0.243 for $N=36$; see Fig. 12).

(iii) The $N=36$ singlet sector of the $J_2=-2$ and $J_4=1$ Hamiltonian has a quasifourfold degeneracy of the ground state (Fig. 13). The lowest energy is a single state and the next energy level, which is immediately above, is threefold degenerate. Because of the large size of the $N=36$ system (compared to the supposed correlation length), we believe that this feature is a particularly valuable information on the spectrum of the infinite system.

In the next paragraphs we analyze these results. First, we argue that these data are not in favor of ''spin-Peierls''-like symmetry breaking. Then we show that a fourfold degeneracy could be of topological origin. Third, we explain why the system is probably not a chiral spin liquid. Eventually, we discuss the link between the MSE spin liquid and some kind of VBS (or Haldane) phase on a square superlattice with four spins in the unit cell.

2. No spin-Peierls symmetry breaking

The $N=36$ singlet sector of the $J_2=-2$ and $J_4=1$ Hamiltonian has a quasidegeneracy of the ground state (Fig. 13). The lowest energy is a single state and the next one is three-fold degenerate (impulsions $\mathbf{k}=\mathbf{A}_{1,2,3}$). As mentioned before, the behavior of the singlet gap to the first $\mathbf{A}_{1,2,3}$ state (Fig. 12) suggests that these two levels are degenerate in the thermodynamic limit. The next pair of energies in $S=0$ may also be seen as asymptotically degenerate $\mathbf{k}=\mathbf{0},\mathbf{k}=\mathbf{A}_i$ states (Fig. 13).

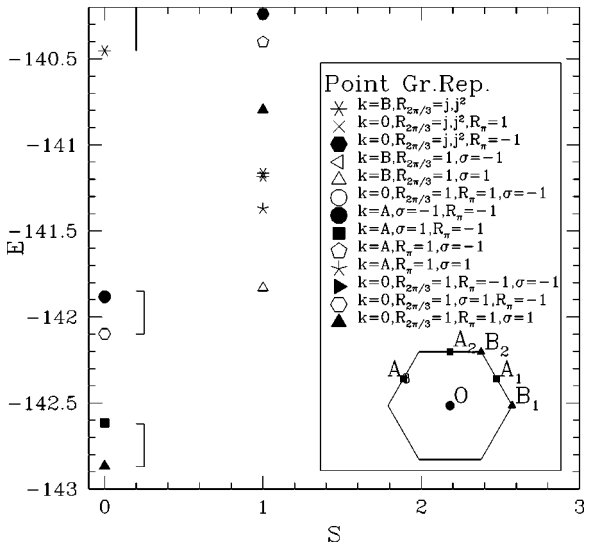

FIG. 13. Lowest-energy levels of the $N=36$ sample ($J_2=-2$ and $J_4=1$) in the sectors of $\mathbf{k}=0$, **A**, and **B**. The symbols represent the quantum number of the different eigenstates. For instance, the ground state ($S=0$, $E=-142.867$) belongs to the trivial representation of the spatial group (solid up triangle, labeled $\mathbf{k}=0$, $R_{2\pi/3}=1$, $R_\pi=1$, $\sigma=1$).

The point is that no pattern gives a fourfold or eightfold degeneracy compatible with the quantum numbers of these four or eight lowest eigenstates. In particular, any long-range-ordered dimer covering leads at least to 12 degenerate states. For bigger patterns (four-site rhombus, for instance) the number of broken symmetries is even larger and so would be the degeneracy. Therefore, the $1+3$ degeneracy of the two first eigenvalues ($\mathbf{k}=0$ and $\mathbf{k}=A_{1,2,3}$) cannot be explained in such a conventional spin-Peierls-like picture.

3. Topological degeneracy

But this degeneracy matches the prediction of a topological degeneracy due to the periodic boundary conditions and to the nontrivial topology of the torus.

Most of the important arguments for this topological degeneracy were proposed by Rokhsar and Kivelson,[30] Read and Chakraborty,[31] and Sutherland[32] but here we sketch a more formal demonstration.

Dimer and loops. The starting point is a dimer representation of the wave function. As remarked by Sutherland,[32] the overlap $\langle C|C'\rangle$ between two normalized valence-bond states C and C' can be diagrammatically computed by constructing their *transition graph*. This graph is obtained by drawing on the same lattice the oriented bonds of C and C'. The result is a set of locally oriented and nonintersecting loops which cover the lattice. Let $n(C\cup C')$ be the number of loops and $x(C\cup C')$ the number of bonds to be reversed for each loop to have alternating bond orientations. The result is

$$\langle C|C'\rangle = 2^{n(C\cup C')-N/2}(-1)^{x(C\cup C')}. \tag{6}$$

As an illustration, consider the trivial case $C=C'$. All loops are of length 2 and their number is $n(C\cup C)=N/2$. Each two-site loop is already alternated and $x(C\cup C)=0$. So we get $\langle C|C\rangle=1$. From the overcomplete family of valence-bond states one can formally extract a (nonorthogonal) basis. In this basis, the ground sate reads

$$|\psi\rangle = \sum_C \psi(C)|C\rangle. \tag{7}$$

The normalization of $|\psi\rangle$ gives

$$\langle\psi|\psi\rangle = \sum_{C,C'} [\psi(C)^\dagger \psi(C') 2^{n(C\cup C')}(-1)^{x(C\cup C')}]. \tag{8}$$

Small loop hypothesis. This equation can be rewritten in term of a sum over the transition graphs, or loop coverings $\mathcal{G}$ of the lattice:

$$\langle\psi|\psi\rangle = \sum_{\mathcal{G}} 2^{n(\mathcal{G})}(-1)^{x(\mathcal{G})}\Gamma(\mathcal{G}), \tag{9}$$

where we defined

$$\Gamma(\mathcal{G}) = \sum_{C,C'/C\cup C'=\mathcal{G}} \psi(C)^\dagger \psi(C'). \tag{10}$$

This is possible because any decomposition $C\cup C'$ of a loop covering $\mathcal{G}$ has the same $(-1)^{x(C\cup C')}=(-1)^{x(\mathcal{G})}$ as well as the same $n(C\cup C')=n(\mathcal{G})$. We now turn to the important hypothesis: we assume that the only graphs $\mathcal{G}$ which contribute to Eq. (9) are those which do not contain any loop surrounding the torus. This statement about the noncontribution of topologically nontrivial loops implies that there should not be any long-distance coherence in the wave function. We stress that this is a much stronger requirement that demanding short dimers (for instance, a valence-bond *solid* or a valence-bond *crystal* state do not fulfill this hypothesis). In the MSE spin liquid all the correlations we measured (spin-spin, chiral-chiral, and dimer-dimer) seem to decay exponentially over a distance ξ and we do nothing but assume that the loops contributing to Eq. (9) have also a finite characteristic length scale. This strong condition implies the fourfold degeneracy of the ground state. We propose the arguments summarized below.

Cuts along the torus and fourfold degeneracy. The idea is now to choose a cut Δ surrounding the torus in one direction. Each valence-bond state C has a number $\Delta(C)$ of bonds crossing Δ and it is possible to change the sign of the configurations C for which $\Delta(C)$ is odd:

$$|\psi'\rangle = \sum_C (-1)^{\Delta(C)}\psi(C)|C\rangle. \tag{11}$$

If the sample has an odd number of sites in the direction perpendicular to Δ and if $|\psi\rangle$ has an impulsion $\mathbf{k}$, it is easy to check that the state $|\psi'\rangle$ has an impulsion $\mathbf{k}'=\mathbf{k}+\mathbf{A}$, where $\mathbf{A}$ is one middle of the boundary of the Brillouin zone (see inset of Fig. 13). But we have also shown[33] that $|\psi'\rangle$ has the same energy as $|\psi\rangle$ provided $|\psi\rangle$ only ''contains'' small loops (hypothesis above). This twofold degeneracy must be extended to *four* when the sample has a $2\pi/3$ rotation symmetry since irreducible representations for wave vector $\mathbf{k}=\mathbf{A}$ are of dimension 3. A similar construction was provided by Wen[38] in the framework of a mean-field model for P- and T-symmetric spin liquids. In Wen's work, a state $|\psi'\rangle$ is

built from the original ground state $|\psi\rangle$ by a singular gauge transformation on the bonds degrees of freedom. This transformation amounts to introduce a $\frac{1}{2}$ flux quantum through a noncontractable loop Δ.

Now we can interpret the $N=36$ singlet sector in the following way: as the system becomes larger than ξ the topologically nontrivial loops grow scarce exponentially with $\sqrt{N}/\xi$. Consequently the lowest singlet eigenstate becomes fourfold degenerate ($\mathbf{k}=0$ and $\mathbf{k}=A_{1,2,3}$). At $N=36$ this topological degeneracy is still not very accurate but we can clearly distinguish two quasiquadruplets.

4. Chiral spin liquid

Some time ago it was suggested that an antiferromagnetic quantum spin liquid could be *chiral* and could break the time-reversal (T) and parity (P) symmetries.[34–36] This scenario was definitely discarded in the case of a simple Heisenberg Hamiltonian on a triangular lattice.[21] The situation on the Kagomé lattice is more ambiguous.[27] In the MSE case, the presence of a gap in the magnetic excitations and the degeneracy of the ground state in the thermodynamic limit would be consistent with a chiral theory. Indeed, Wen[37] argues that an incompressible chiral fluid should have a $2k^g$-fold vacuum degeneracy on a manifold of genius g (but this is not specific to chiral models: one also finds a 2^g topological degeneracy in P- and T-symmetric models[38]). On the other hand, as underlined before, the MSE does not support LRO in the chiral parameter $\kappa=2(\vec{S}_1\times\vec{S}_3)\cdot\vec{S}_2$. Therefore, the only possibility would be a hypothetical ''chiral spin-liquid'' ground state[35,36] where the expectation value of a cyclic permutation operator $P_{i_1,i_2,i_3,\ldots,i_n}$ acquires a nonzero imaginary part on large loops, $i_1,i_2,i_3,\ldots,i_n$. In such theories elementary excitations are unconfined spin-$\frac{1}{2}$ excitations. The spectra of $N=27$ and $N=28$ are the largest pair of consecutive sizes we diagonalized and are believed to be close to the asymptotic limit. Their comparison does not plead in favor of this unconfined spinon hypothesis: the ground-state energy per site of $N=27$ ($E^{S=0}/N=-3.919$) is slightly lower than the first triplet energy per site of $N=28$ ($E^{S=1}/N=-3.918$ and $E^{S=0}/N=-3.963$). This is rather a signature of elementary *spin-1 excitations* and makes the chiral scenario unlikely.

5. VBS/Haldane system

We have shown, so far, that the MSE spin liquid is characterized by a low ground-state degeneracy. For half-integer spins in one dimension, the Lieb-Shultz-Mattis[39] (LSM) theorem forces the ground state to be degenerate or gapless. Some attempts to generalize it in two dimensions[40] suggest that a ground-state degeneracy could also be generic in a (half-integer) gapped state in two dimensions. From this point of view, our results in the MSE case are not unexpected. But such a degeneracy is usually associated with a spontaneous breaking of a discrete symmetry, say, translation, and a dimer or plaquette local order parameter. If our analysis of the $N=36$ spectrum is correct, such a spin-Peierls phenomenon is absent. Without any evidence of a simple local order parameter, the topological point of view is natural and states that a ground-state degeneracy can occur without any local order parameter breaking a discrete symmetry (a famous example is the Laughlin wave function, the discrete degeneracy of which depends on the space topology[41]). However, the translation symmetry is almost certainly broken in the MSE case (at least four states with different impulsions are asymptotically degenerate) and one should be careful before excluding the possibility of *any* kind of LRO. In a search for an alternative to the topological degeneracy, we looked for explicit wave functions (for half-integer spin) with a low degeneracy and the minimum number of broken spatial symmetries to compare with numerical results.

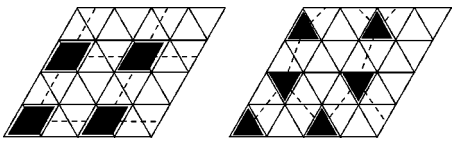

FIG. 14. Left: black rhombus represent the $S=2$ spins of the VBS wave function. They form a square lattice (dashed lines). Right: honeycomb superlattice of three-site plaquettes on the triangular lattice. There are 18 different ways to place this honeycomb superlattice on the triangular one (3×2 translations and three rotations).

For high spins matching the coordination number ($2S=z$) the VBS wave function is nondegenerate. When this criterion is not satisfied, nevertheless, the VBS procedure can help to write wave functions with few broken symmetries. The idea is to chose a superlattice with n spins in the unit cell and of coordination number $z=n$. On the superlattice, a unique VBS state is written by identifying the n spins of a cell as a larger spin $S=n/2$. The state we obtained has a degeneracy which is the number of possibilities to define a superlattice L over a real (triangular) lattice. Consider the $S=2$ VBS wave function for the square lattice. It is mapped onto the spin-$\frac{1}{2}$ triangular lattice by identifying the $S=2$ spins of the square lattice to four spins $s=\frac{1}{2}$ (on a rhombus) of the triangular one [Fig. 14(a)]. The choice of the position of the square superlattice is done among 12 different possibilities: a configuration can be translated at four different places and rotated in three directions. One should remark that these states do have some long-ranged order. Let Π_a be the projection operator of the rhombus a in its $S=2$ subspace. By construction, the eight-point correlation function $\langle\Pi_a\Pi_b\rangle$ is long ranged.

We computed the ground-state energy inside this 12-dimensional VBS subspace on a small system ($N=12$ at $J_4=1$ and $J_2=-2$) and found a good variational energy. The exact ground-state energy is $E/N\simeq-4.128$ and the VBS energy is $E/N=-3.75$. The energy scale is given by the energy of the ferromagnetic state ($E/N=0$), and the energy of the ground state $E/N=-3$ for classical spins. This variational result is *the best achieved so far* and is even much better than the Schwinger-boson energy for this Hamiltonian [the Schwinger-boson solution is a two-sublattice (NLRO) collinear state with $E/N=-2.96$]. The reason for this competitive energy is that the VBS construction naturally provides some local ferromagnetism inside a plaquette which lowers $J_2P_{1,2}$ and some antiferromagnetism at larger dis-

tance (between neighboring rhombus) which ensures a low $J_4(P_{1,2,3,4}+\text{H.c.})$. When the size of the unit cell is varied, one tunes the strength of the antiferromagnetic correlations at short distance. For instance, it is possible to enhance it if we start from the wave function of the $S=3/2$ honeycomb lattice [Fig. 14(b)], where the unit cell has only three sites. In this case we find an energy slightly higher ($E/N=-3.42$ on 12 sites). On the other hand, varying the ferromagnetic coupling J_2 in the Hamiltonian could bring the ground state closer to a VBS wave function.

The 12 VBS states are not coupled by any local Hamiltonian in the thermodynamic limit, and should therefore be degenerate in an infinite system. In a theory where all excitations are gapped, the low-energy physics (except for possible edge states) is determined by the degenerate ground state. Therefore, this 12-fold degeneracy characterizes the fixed point and we expect the same degeneracy in the MSE problem if it belongs to this universality class. Unfortunately the quantum numbers only partially coincide with the lowest eigenstates found in the $N=36$ spectrum. So despite a good variational energy on $N=12$, these particular trial states do not provide a quantitative explanation of the fourfold or eightfold degeneracy observed on 36 sites. However, the family of these extended VBS states certainly captures a part of the local constraints imposed by frustrating MSE couplings. Furthermore, we cannot *completely* exclude that the $N=36$ might not be a faithful picture of the infinite system spectrum and that the ground state could have a complex valence-bond solid order of the type we have just described.

V. SUMMARY AND CONCLUSIONS

We analyzed the spin-liquid phase of MSE model on the triangular lattice. Due to important frustration, LRO is destroyed by quantum fluctuations at zero temperature. The system has short-ranged correlations: $\langle \vec{S}_i \cdot \vec{S}_j \rangle$, dimer-dimer, and chiral-chiral correlations probably decay exponentially with distance. The spectrum has a spin gap and the comparison between odd and even sample pleads in favor of spin-1 excitations. As for the spatial symmetries and degeneracy of the ground state (presumably 4 or 8), they provide evidence of no spin-Peierls or simple plaquette order. This is a generic feature in systems where the spin matches the coordination number ($2S=z$) and where a VBS wave function can be constructed, but it is unconventional for spin $\frac{1}{2}$. We proposed two interpretations. The first possibility is a VBS or Haldane-like phase. We constructed such a wave function, which is not a tensor product of plaquette states. Present numerical data on the ground-state symmetries do not completely agree with this particular trial state, but because of its very low variational energy, such a scenario cannot be excluded. Second, this degeneracy might be a consequence of the nontrivial topology implied by periodic boundary conditions. We emphasized that it must be the case if the system has absolutely no long-ranged coherence.

This spin-liquid phase might be the very first magnet with a ''disordered'' and gapped quantum ground state with no simple local order parameter in two dimensions. From this point of view it can be seen as a prototype of the RVB state as was proposed by Anderson.[17]

ACKNOWLEDGMENTS

We have benefited from very interesting discussions with K. Kubo and T. Jolicoeur. Computations were performed on CRAY C94, C98 and T3E-256 at the Institut de Développement des Recherches en Informatique Scientifique of C.N.R.S. under Contract Nos. 960076/964091 and on CRAY T3E-512 of the Zentralinstitut für Angewandte Mathematik, Forschungszentrum Jülich.

[1] D. J. Thouless, Proc. Phys. Soc. London **86**, 893 (1965).
[2] M. Roger, C. Bäuerle, Yu. M. Bunkov, A.-S. Chen, and H. Godfrin, Phys. Rev. Lett. **80**, 1308 (1998).
[3] M. Roger, Phys. Rev. B **30**, 6432 (1984).
[4] S. Chakravarty, S. Kivelson, C. Nayak, and K. Volker, cond-mat/9805383 (unpublished).
[5] G. Misguich, B. Bernu, C. Lhuillier, and C. Waldtmann, Phys. Rev. Lett. **81**, 1098 (1998).
[6] D. J. Klein, J. Phys. A **15**, 661 (1982).
[7] C. K. Majumdar and D. K. Ghosh, J. Math. Phys. **10**, 1399 (1969).
[8] H. Schulz and T. Ziman, Europhys. Lett. **18**, 355 (1992), and references therein.
[9] M. E. Zhitomirsky and K. Ueda, Phys. Rev. B **54**, 9007 (1996).
[10] N. Read and S. Sachdev, Phys. Rev. Lett. **62**, 1694 (1989).
[11] N. Read and S. Sachdev, Phys. Rev. B **42**, 4568 (1990).
[12] N. Read and S. Sachdev, Phys. Rev. Lett. **66**, 1773 (1991).
[13] I. Affleck, T. Kennedy, E. H. Lieb, and H. Tasaki, Phys. Rev. Lett. **59**, 799 (1987).
[14] F. D. M. Haldane, Phys. Rev. Lett. **61**, 1029 (1988).
[15] J. Chayes, L. Chayes, and S. Kivelson, Commun. Math. Phys. **123**, 53 (1989).
[16] F. Figueirido, A. Karhede, S. Kivelson, S. Sondhi, M. Rocek, and D. S. Rokhsar, Phys. Rev. B **41**, 4619 (1990).
[17] P. W. Anderson, Mater. Res. Bull. **8**, 153 (1973).
[18] K. Kubo and T. Momoi, Z. Phys. B **103**, 485 (1997).
[19] T. Momoi, K. Kubo, and K. Niki, Phys. Rev. Lett. **79**, 2081 (1997).
[20] G. Misguich, B. Bernu, and C. Lhuillier, J. Low Temp. Phys. **110**, 327 (1998).
[21] B. Bernu, C. Lhuillier, and L. Pierre, Phys. Rev. Lett. **69**, 2590 (1992); B. Bernu, P. Lecheminant, C. Lhuillier, and L. Pierre, Phys. Rev. B **50**, 10 048 (1994).
[22] P. Lecheminant, B. Bernu, C. Lhuillier, L. Pierre, and P. Sindzingre, Phys. Rev. B **56**, 2521 (1997).
[23] The softest magnon has a total energy $E_{min}=c|\mathbf{k}_{min}|$ where c is the slowest spin-wave velocity and $\mathbf{k}_{min}\sim 1/\sqrt{N}$ is the smallest wave vector allowed by the periodic boundary conditions on the finite size sample. This gives $E_{min}\simeq c/\sqrt{N}$.
[24] With periodic boundary conditions, the spin $\vec{S}_i$ at site **i** interacts with the spin $\vec{S}_j$ at site **j**. Using the wave vector **q** to twist the system makes the rotated spin $\mathcal{R}^z_{\mathbf{q}\cdot\mathbf{i}}[\vec{S}_i]$ interact with $\mathcal{R}^z_{\mathbf{q}\cdot\mathbf{j}}[\vec{S}_j]$. $\mathcal{R}^z_\theta$ is the rotation of angle θ about the quantification axis z. Such a Hamiltonian is no longer SU(2) invariant when $\mathbf{q}\neq 0$: $\vec{S}^2_{tot}=(\Sigma_i \vec{S}_i)^2$ is no longer a conserved quantity but S^z_{tot} commutes with the twisted Hamiltonian.

[25] A simple way to evaluate how the the **v** step is ''frustrated'' by the periodic boundary conditions of the torus is to consider a closed loop starting from the origin: $O, O+\mathbf{v}, O+2\mathbf{v}, \ldots, O+(n-1)\mathbf{v}, O$. We associate frustration with the *winding number* of this closed curve. The minimum number is 1: by successive translation of **v** we are back to the origin after winding one time around the torus. We make the assumption that unphysical effects due to the finite size of the torus are smaller in the direction where the winding number is the smallest. Given the distance d, the relevant $\langle \vec{S}_i \cdot \vec{S}_j \rangle$ is thus obtained in the direction which gives the topologically simplest loop.

[26] If the system is invariant under rotation of $2\pi/3$, $\langle \Psi | d_{i,j} | \Psi \rangle$ only depends on the bond length $|j-i|$.

[27] C. Waldtmann, H. U. Everts, B. Bernu, C. Lhuillier, P. Sindzingre, P. Lecheminant, and L. Pierre, Eur. Phys. J. B **2**, 501 (1998).

[28] Systems with the lowest ground-state energy per site turn out to be those with wave vectors $\mathbf{k}=\mathbf{A}$, **B**, and **B/2** in their first Brillouin zone. An illustration of this sensivity to the shape is provided by the two $N=24$ systems of Fig. 11. The more stable $N=24$ system is the 6×4 torus (which possesses the four wave vectors mentioned and $E/N=-4.03$). It can be compared with the most compact 24-site torus (label $24'$ in Fig. 11 and open square at $N=24$ in Fig. 10). The latter has only one $\mathbf{k}=\mathbf{A}$ vector and is more frustrated: $E/N=-3.88$. The same behavior was observed for 12 and 20 sites.

[29] Notice that the situation would be different in the case of NLRO. The finite-size corrections of the ground-state energy per site are proportional to $N^{-3/2}$ (linear spin-wave result). The energies of the different families of samples (those which frustrate the LRO and those which do not) would intercept linearly at $N=\infty$ in a plot of E/N versus $N^{-3/2}$. As for the spin gap, it would vanish as N^{-1}: this is definitely inconsistent with present results (Fig. 10).

[30] D. S. Rokhsar and S. A. Kivelson, Phys. Rev. Lett. **61**, 2376 (1988).

[31] N. Read and B. Chakraborty, Phys. Rev. B **40**, 7133 (1989).

[32] B. Sutherland, Phys. Rev. B **37**, 3786 (1988).

[33] G. Misguich, Ph.D thesis. Université Paris VI, 1999.

[34] V. Kalmeyer and R. B. Laughlin, Phys. Rev. Lett. **59**, 2095 (1987).

[35] V. Kalmeyer and R. B. Laughlin, Phys. Rev. B **39**, 11 879 (1989).

[36] X. G. Wen, F. Wilczek, and A. Zee, Phys. Rev. B **39**, 11 413 (1989).

[37] X. G. Wen, Phys. Rev. B **40**, 7387 (1989).

[38] X. G. Wen, Phys. Rev. B **44**, 2664 (1991).

[39] E. Lieb, T. Shultz, and D. Mattis, Ann. Phys. (N.Y.) **16**, 407 (1961).

[40] I. Affleck, Phys. Rev. B **37**, 5186 (1988).

[41] X. G. Wen and Q. Niu, Phys. Rev. B **41**, 9377 (1990).

[42] T. Momoi, H. Sakamoto, and K. Kubo, Phys. Rev. B **59**, 9491 (1999).